FACTA UNIVERSITATIS
Series:**Mechanical Engineering**
https://doi.org/10.22190/FUME201230028A

Original scientific paper

TAGUCHI OPTIMIZATION OF MULTIPLE PERFORMANCE CHARACTERISTICS IN THE ELECTRICAL DISCHARGE MACHINING OF THE TIGR2

Sıtkı Akıncıoğlu

Department of Machine Design and Construction, University of Düzce, Turkey

Abstract. *Electrical discharge machining (EDM) provides many advantages for the shaping of metallic materials. It also provides better surface quality for Ti alloys used in the defense industry. In this study, experiments were carried out with different EDM parameters using the Titanium (Gr2) alloy. A number of novel industrial processes have been developed as a result of advances in technology. For a product to be developed, these novel approaches must be utilized to determine optimum parameters. The Taguchi method was applied in the experiments with EDM. The impact the test parameters had on the performance characteristics of tool wear rate, material removal rate, depth, and surface roughness were analyzed by the variance analysis (ANOVA). Quadratic regression analyses were carried out to reveal the correlation between the experimental results and the predicted values. According to the ANOVA results for material removal rate (MRR), tool wear rate (TWR), depth, and surface roughness, the most effective factor was amperage, at 99.66%, 99.56%, 87.95%, and 81.12%, respectively. The best value for average surface roughness was determined to be 3.29 µm obtained at 120 µs time-on, 8 A, and 40 µs time-off.*

Key Words: *Electrical discharge machining (EDM), Taguchi method, Optimization, Titanium (Gr2), Material removal rate*

1. INTRODUCTION

Electrical discharge machining (EDM) provides many advantages in the processing of specially shaped workpieces, irrespective of material strength or hardness [1]. The effectiveness of EDM is independent of the mechanical properties of the workpiece [2]. However, EDM has a lower processing speed than that of traditional machining methods. Furthermore, because of the cracks and micro-pits formed in the recast layer as a result of rapid cooling, less surface accuracy and a shorter cutting-tool life are obtained in molds

Received December 30, 2020 / Accepted March 10, 2021
Corresponding author: Sıtkı Akıncıoğlu
Department of Machine Design and Construction, University of Düzce,Gümüşova, Düzce, Turkey
E-mail: sitkiakincioglu@duzce.edu.tr

or machine parts, and thus, EDM has a low MRR and poor processing precision. Therefore, more detailed investigations are needed in order to overcome these disadvantages [3, 4].

The advantages of titanium alloys are recognized in many industrial sectors, including the defense, aerospace, and automotive industries, as well as for power generation, desalination, architecture, marine, and medical applications because of their high corrosion resistance, high strength, low specific gravity and high thermal resistance. Titanium Gr 2 is pure commercial alpha titanium. Titanium Grade 2 materials contain a minimum of 99% titanium elements. These alloys have very good corrosion resistance, mechanical strength and low weight, besides being extremely resistant to chemical environments such as alkali environments, organic acids and compounds, aqueous salt solutions and hot gases. Titanium Grade 2 materials are frequently used in the chemical industry, marine vehicles, aviation vehicles and medical parts. The selection of the parameters during machining affects surface quality and processing costs [5]. Difficult-to-process titanium alloys can be processed easily with EDM [2]; however, the speed of processing and the quality of the surface must be increased. These development efforts are expensive due to a high cost of the titanium alloy, the long duration of the EDM process, and the need for extra testing. The Taguchi design optimizes a response variable with various control factors and noise factors. It is an efficient and inexpensive experimental design method using fewer resources than full factorial design. Because the Taguchi method greatly reduces the number of trials necessary for the experiments, in recent years, its advantage has been increasingly recognized [6]. In many studies, researchers have successfully optimized the parameters in the EDM process using the Taguchi method. Manisha et al. [7] machined the titanium alloy from the test material by using different parameters in the EDM optimized with the Taguchi method (L_{25}). The parameters used in the experiments were determined as pulse duration (time-on), duty factor, discharge current [amperage (A)] and gap voltage (Vg). The analysis of variance (ANOVA) test showed that the most effective parameter for material removal rate (MRR) was duty (52.87%). According to the signal/noise (S/N) ratios, the optimum parameters were calculated as tone (30 μs), duty factor (9), current (50 A) and Vg (6 V). Vijay et al. [8] used the L_9 orthogonal array Taguchi method to optimize the parameters used in the processing of a titanium alloy (Ti6Al4V) in EDM. The processing parameters were determined as three different on-time pulses, three different off-time pulses, fluid pressure, and voltage. They investigated material wear loss, tool wear loss, and surface roughness values and successfully determined the optimum parameters for MRR, tool TWR, and surface roughness. Sunil et al. [9] analyzed the results for MRR, TWR and surface roughness obtained by processing the titanium alloy Ti-6Al-4V using EDM *via* the Taguchi experimental design (L_{18}). The parameters used in the experiments were selected as duty cycle, amperage, working time, electrode, voltage, retraction distance, pulse duration, and liquid pressure. They found that the most effective parameter for MRR was the duration of the pulse (tone), the increase of the washing pressure and the increase of the surface roughness. Jeavudeen et al. [10] investigated the EDM machining performance of Titanium and HSS material of duty factor and the mixture of Alumina powder to dielectric. Taguchi's L9 orthogonal array was used to optimize its effect on MRR and tool wear index (TWI) in the EDM processing. The MRR results show that the current and dust concentration increase the material removal rate of the HSS and Titanium workpiece. The TWI of the HSS sample was also found to be higher than the

Titanium sample. Gaikwad et al. [11] machined EDM and NiTi alloy using a copper electrode. In their work, they discussed process parameters such as gap current, pulse on time, pulse off time. Using the Taguchi method, they found important process parameters affecting tool electrode and workpiece electrical conductivity, pulse on time, gap current, tool wear rate, and material removal rate. As a result of the study, they found the optimum tool wear rate of 0.031 mm^3/min and the optimum material removal rate of 6.31 mm^3/min. Nagaraju et al. [12] machined 17-7 PH stainless steel using the EDM method. They used current, pulse on time, discharge voltage Surface Roughness, Overcut and Clearance in Electrical as processing parameters. They used Taguchi L9 orthogonal array to optimize parameters. Gugulothu et al. [13] investigated the effect of the Ti-6Al-4V alloy on the electric discharge treatment of drinking water as the dielectric liquid and graphite powder concentration. They examined the effects of discharge current, pulse on time, pulse off time and graphite powder concentration parameters on properties such as material removal rate, surface roughness and recast layer thickness. They used the Taguchi method for optimization of parameters. It has been found that the discharge current is the most important parameter affecting MRR, SR and RLT. Also, the dust concentration is less important. Lin et al. [14] examined the performance characteristics of SKD11 tool steel using EDM. The machining parameters were optimized with respect to the multiple performance characteristics. The experimental results demonstrated the effectiveness of this approach.

Difficult materials can be easily shaped with EDM. This process has a low metal removal rate and a high tool wear rate. For this reason, this study aimed to increase the metal removal rate and reduce the electrode consumption without reducing the surface quality of the Titanium GR2 alloy. Many superalloys have been machined with EDM. However, research on EDM of pure titanium alloy Gr2 quality alloy is very limited. Kumar et al. [15] investigated the processing of biomedical Titanium alloys using EDM and WEDM. In their research, they examined many studies on the EDM processing of titanium alloys. According to their results, it is very advantageous to process titanium alloys with EDM. However, he states that the role of the EDM process for surface modification of Titanium Biomaterials is still in the experimental phase. Nimbalkar et al. [16] also reported that many studies need to be done to process titanium with EDM. Gupta et al. [17] also explained that there is room for improvement in processing Titanium with EDM. He also reported that the Taguchi Method can be used in the complex EDM optimization of Titanium. This study aims at increasing surface quality, reducing electrode consumption and shortening the processing time.

Thanks to the EDM method, the machining of difficult materials has been made easy. Although the EDM machining is a time-consuming method, it can also be cost-effective. The studies have been done on titanium super alloy before surface quality, MRR and TWR of the titanium Gr2 the workpiece is not at the desired level. The studies on the machining of titanium super alloys with EDM have been limited. Comprehensive studies are required to increase the surface quality of the Titanium Gr2 alloy workpiece and to reduce the machining costs. In this current study, the effects of the parameters of pulse duration (time-on), waiting time (time-off), and amperage, on tool wear rate, cutting depth, and surface roughness were optimized by using the Taguchi method in the machining of the titanium alloy in EDM. It provided a comprehensive analysis of the EDM machining of Titanium Gr2 using both the Taguchi method and the Gray Relational

Analysis. In addition, the ANOVA and regression analyses were performed to interpret the results more accurately.

2. Material and Methods

2.1 Electrical discharge machine

The King ZNC - K - 3200 Electro - discharge machine (Fig. 1) was used for the experimental trials in the study.

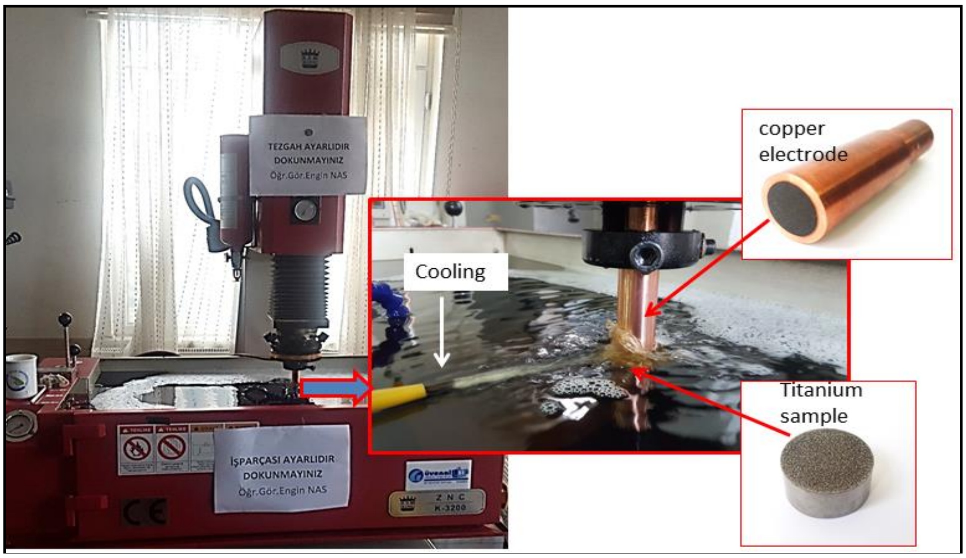

Fig. 1 Electro-discharge machine used in the experimental work

The electrical discharge machining process is a technique using sparks produced by electrical discharge to manufacture workpieces in accurate dimensions and shape [18]. The TWR and MRR are calculated using standard arithmetic equations. The differences in the weights of the workpiece and the electrode per minute, before and after machining is carried out, are used in the calculation of the MRR and TWR, respectively [19]. The formulae for calculation of the MMR and TWR are given as (Eq. 1) and (Eq. 2), respectively [18].

$$\mathrm{MRR} = \left[\frac{(W_i - W_f)}{t}\right] \tag{1}$$

Here, MRR is the material removal rate (g/min), W_i is the initial weight of workpiece (g), W_f is the final weight of workpiece (g), and t is the duration of the experimental trial (min).

$$\mathrm{TWR} = \left[\frac{(T_i - T_f)}{t}\right] \tag{2}$$

Here, TWR is the tool wear rate (g/min), T_i is the initial weight of electrode (g), T_f is the final weight of electrode (g), and *t* is the duration of the experimental trial (min).

2.2 Material and electrode selection

In the experimental work, nine 10 × 10 mm pieces of titanium (Gr2) alloys were used. Table 1 presents the workpiece material chemical composition and Table 2 gives its mechanical and physical characteristics.

Table 1 Chemical composition of titanium Gr2

C	Fe	N	O	H	Titanium
0.10	0.20	0.03	0.25	0.015	Balance

Table 2 Physical and mechanical properties of Titanium Gr2

	Properties	Values
1	Density, (g/cm^3)	4.51
2	Melting point, (°C)	1660
3	Electrical resistivity, 10-6 (ohm•cm)	56
4	Thermal conductivity, (W/m•°C)	20.8
5	Specific heat, (J/Kg•°C)	520
6	Tensile strength, (ksi)	50
7	Yield strength, (ksi)	40
8	Stretching, (%)	20
9	Hardness, (HRB)	82

The electrolytic copper electrode used in the EDM tests was 25 mm in diameter, with a density of 8.9 g/cm^3 (Table 3).

Table 3 Properties of the electrode

	Properties	Values
1	Melting point (°C)	1083
2	Elastic modulus (N/mm2)	1.23×105
3	Poisson’s ratio	0.26
4	Density (g/cm^3)	8.9

2.3 Scanning electron microscopy and measurement of surface roughness and weight

Scanning electron microscopy (SEM) was performed using the FEI Quanta FEG 250 instruments to examine and measure the built-up edge (BUE) occurring on the cutting tool. A MAHR meter was used to measure the surface roughness values at room temperature. In order to minimize errors that may arise during the measurement, the surface roughness has been measured from five different locations. The measurement length was determined as 8 mm. A cut-off of 0.8 mm and a sampling length of 5.6 mm were set for the measurement of the surface roughness values during the machining of the workpiece. A Radwag precision scale (0.001 g) was used to measure the test sample weight loss.

2.4 Taguchi method

The Taguchi design of experiments (DOE) is used extensively in the industrial sector as well as in the academic field as a method of determining the parameters that are the most effective in accordance with the experimental results. Experimental design using the Taguchi method is a powerful statistical method for analyzing the interaction among variables [20]. The Taguchi method enables manufacturers to reduce the design and production time needed to develop their products, thus lowering costs and consequently, increasing their business profits [6, 21]. Moreover, the variables that are otherwise unaccountable and uncontrollable using conventional experimental design can be controlled with the Taguchi DOE. The objective function values are converted *via* the Taguchi method to a signal/noise (S/N) ratio, which allows the performance characteristics of the control factor levels to be measured against these factors. The S / N ratio expresses the relation of the strength of the signal to that of the noise [22]. The Taguchi test design measured each control factor combination for surface roughness (Ra) and the control factors were optimized using the S/N ratios. For the calculation of the S/N ratios, the objective functions, according to the characteristic type, are expressed as “the nominal is best” (Eq. (3)), “the largest is best” (Eq. 4) and “the smallest is best” (Eq. (5)) [23].

$$\text{The nominal is best: } \frac{S}{N} = 10\log\left(\frac{\bar{y}}{S_{\bar{y}}^2}\right) \tag{3}$$

$$\text{The largest is best: } \frac{S}{N} = -10\log\frac{1}{n}\sum_{i=1}^{n}\frac{1}{y_i^2} \tag{4}$$

$$\text{The smallest is best: } \frac{S}{N} = -10\log\frac{1}{n}\sum_{i=1}^{n}\frac{1}{y_i^2} \tag{5}$$

The aim of this study was to minimize surface roughness, MRR, and TWR, and to use the "the smallest is best" quality characteristic in (Eq. 5).

2.5 Parameters and levels

Table 4 shows the levels of the parameters of time-on, time-off, and amperage that were used for the experimental study. A constant cutting depth of 0.5 mm was used in the experiments. Time-on, Time-off and Amperage values were determined by making use of the studies. These values have been tested primarily with preliminary experiments. The values obtained later were designed using the Taguchi Method. These parameter levels indicated that the L9 Taguchi orthogonal array should be chosen as the most suitable for this study (Table 5).

Table 4 Test parameters and levels

Parameters	Symbols	Units	Level 1	Level 2	Level 3
Time-on	A	(μs)	120	122	124
Time-off	B	(μs)	40	44	48
Amperage	C	(A)	8	12	16

Table 5 Taguchi orthogonal array design L_9

Exp. No.	Factor A	Factor B	Factor C
1	1	1	1
2	1	2	2
3	1	3	3
4	2	1	2
5	2	2	3
6	2	3	1
7	3	1	3
8	3	2	1
9	3	3	2

3. Results and Discussion

3.1 Experimental results

After a review of the relevant literature studies, the parameters were chosen accordingly for the use in the experiments. Table 6 shows the results of the experimental study. According to these results, wear loss of the copper electrode and titanium workpiece material, cutting depth and average surface roughness values were evaluated.

Table 6 Experimental results

Exp. No.	Time-on (μs)	Time-off (μs)	Amperage (A)	Total processing time (min)	Electrode wear loss (g)	Material wear loss (g)	Electrode height difference (mm)	Material height difference (mm)	Average surface roughness Ra (μm)
1	120	40	8	511.06	0.036	0.441	0.16	0.50	3.29
2	120	44	12	207.70	0.045	0.368	0.16	0.41	4.38
3	120	48	16	126.20	0.060	0.476	0.10	0.44	5.40
4	122	40	12	278.36	0.068	0.483	0.10	0.48	4.12
5	122	44	16	118.56	0.056	0.443	0.12	0.30	5.14
6	122	48	8	705.50	0.047	0.517	0.12	0.50	4.06
7	124	40	16	118.56	0.060	0.449	0.10	0.40	5.17
8	124	44	8	666.13	0.048	0.547	0.10	0.50	4.24
9	124	48	12	313.90	0.069	0.477	0.20	0.30	4.61

Since the electrical conductivity of the titanium material is low, it took a long time to remove 0.5 mm of material. After completion of the experiments, the maximum time (705.50 min) to achieve the treatment was seen in the 6th experiment, while the shortest processing time (118.56 min) was reached in the 5th and 7th experiments. It was recognized that the processing time decreased with the increase of amperage [3]. The 5th and 7th test parameters could be chosen as rough machining for this material in order to reduce the processing time. The minimum amount of electrode wear (0.036 g) was observed in the 1st experiment and the maximum electrode wear (0.069 g) in the 9th. It can be seen that the selected parameter values were not compatible with one another due to a high amount of electrode wear. The amount of electrode wear was less than that of material wear. The material wear amount and processing time were also parallel. The lowest average surface roughness was obtained under the processing conditions of the 1st experiment (120 μs time-on, 40 μs time-off, 8 A for 511.06 min). From this result, the processing time was found to be average. It appears that there was no specific relationship between the machining time and the surface roughness. Lin et al. [3] achieved similar results in processing titanium using EDM. Surface quality decreased with the increase of amperage.

3.2 Surface analysis

Many parameters such as pulse current, impact time, tool electrode and workpiece materials are effective on the surface integrity of the EDM applied surface [24, 25]. Examination of profilometry and SEM images was used to determine the average surface roughness values achieved *via* the experiments. The best surface roughness values were achieved in the 1st experiment (8 A, 120 μs time-on, and 40 μs time-off). The highest surface roughness value (5.40 μm) was obtained in the 4th experiment (16A, 120 μs time-on, and 48 μs time-off). It can be concluded that the increase of the amperage value had a negative effect on the surface roughness. The formation of large craters as a result of a high amperage discharge adversely affected the surface roughness. The reason for the formation of surface cracks is tensile stress caused by shrinkage of the molten material during cooling of the workpiece surface after the spark. Surface cracks occur because the tensile stress of the material exceeds the final tensile stress in the white layer. Increasing amperage increases pits and micro holes. Thus, its amperage must increase in order to increase the MRR during electrical discharge. It creates larger and deeper craters and holes as the amperage increases [24, 26].These results are consistent with those of other studies [27]. Although amperage discharge negatively affected the surface, it shortened the machining time. Fig. 2 shows the average surface roughness (Ra) values as 3D images obtained *via* profilometer, with the low Ra values indicated in green and yellow. In contrast to the deeper pits, the highest Ra values are indicated by the red peaks formed on the surface. With the increase of the amperage, the surface roughness value was clearly increased [7].

The surface topography varied significantly depending on the electrical parameters of time-on, time-off, and amperage. The most important factors in the deterioration of surface quality were amperage and the time-on. With the increase of the time-on and amperage, an increase in the crater size was observed in the surface area. During the short time-on, electrical sparks were found to form small craters on the surface of the workpiece [28].

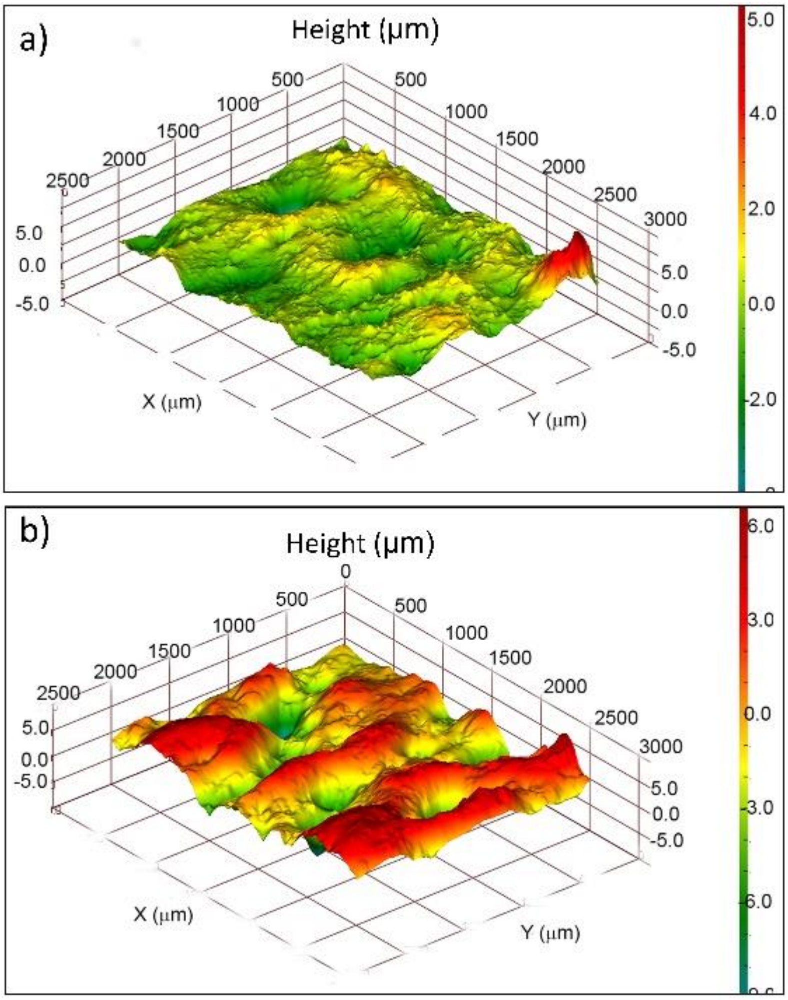

Fig. 2 3D surface profile of test specimens: a) 1st sample, b) 3rd sample

3.3 Microstructural analysis

The very high temperatures generated at the spark point were a result of the energy discharged during the EDM process, and caused the evaporation and obliteration of portions of the sample surface. With each discharge flow, spherical particles were formed in the crater, and micro fractures and crater edges of various sizes were formed on the machining surfaces (Fig. 3) [29]. Examination of the SEM images of the machined surface showed that the first experiment yielded the lowest surface roughness. The low amperage (8 A) caused small gaps in the surface. In the 3rd experiment, the highest surface roughness value was obtained by the increase of amperage (16 A). This can be explained by the growth of the gaps in the surface profile and the heat input rates [30]. It has been reported in the literature that the craters formed on the surface grow with the increase in the amount of amperage [27]. The SEM images of the machined surfaces show that the surface roughness of the1st sample (Fig. 3a) is better than that of the 3rd sample (Fig. 3b). The SEM cross-section views (Fig. 4) show the craters, micro peaks and material residue appearing on the surfaces, and a white layer (recast layer) can be seen [31]. The high amperage caused large craters to form. The white layer occurred due to sudden heating and cooling. This was the result of residual tensile stresses in the warming zone which caused surface fractures and surface defects on the workpiece [27]. The intensity and depth of surface cracks may vary depending on the machining parameters. It was found that the cracks increased with increasing amperage levels. The cause of this increase in the cracks was the surface tension which occurred in the material due to a high temperature formation during the time-on [32].

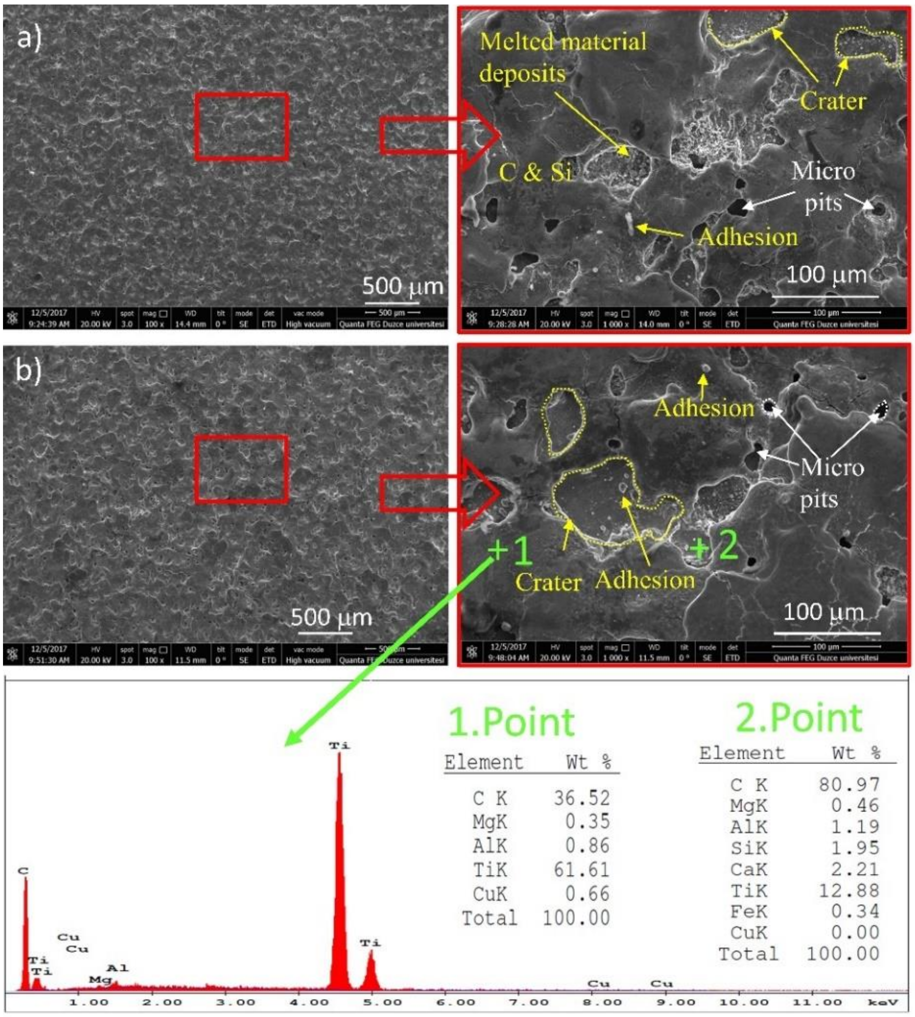

Fig. 3 SEM view of test specimens and EDAX analysis: a) 1st sample, b) 3rd sample

The recast layer (white layer) (Fig. 4) is the outer region of the heat affected zone. It is a layer formed by the overlapping of the molten and solidified workpiece material. This heat-affected solidified layer is a white layer that can be seen adjacent to the titanium [27]. These layers occurred due to a cut in the amperage. Some of the particles of the adherent material were removed by the dielectric fluid. Without moving away, some of them cooled down and amassed on the material to form a white layer [28].

The thermal under the workpiece top surface is dissipated more slowly than the top surface subjected to rapid cooling due to dielectric flow. Thermal transformation depends on the thermal behavior of the workpiece. Titanium alloys have lower thermal conductivity compared to steels. Under the white layer formed on the surface of the workpiece, a tempered layer is formed in the heat affected area. Finally, under the top two layers is the area of the workpiece that is not affected by the process. Among these three layers, the white layer is the most important one because of its direct contact with the liquid and gap environment. The thickness of the recast layer varies according to the EDM processing parameters [24, 33]. The formation of Titanium carbides caused by the white layer gives rise to hardness of the recast layer.

It has been reported that the average thickness of the reformed layer is increased by increasing the amperage. As the amperage increases, the surface temperature reaches the melting point faster. Thus, the material removal rate increases. Increasing the amount of the melted particle increases the solidified particle ratio. Thus, the white layer formation also increases. As the pulse on time increases, so does the average thickness of the recast layer. Thus, with the pulse on time increasing, more thermal energy is transferred to the sample surface during electrical discharge in a single pulse. When the pulse on time increases, the melting regions penetrate deeper and cause more the MRR formation [24, 34].

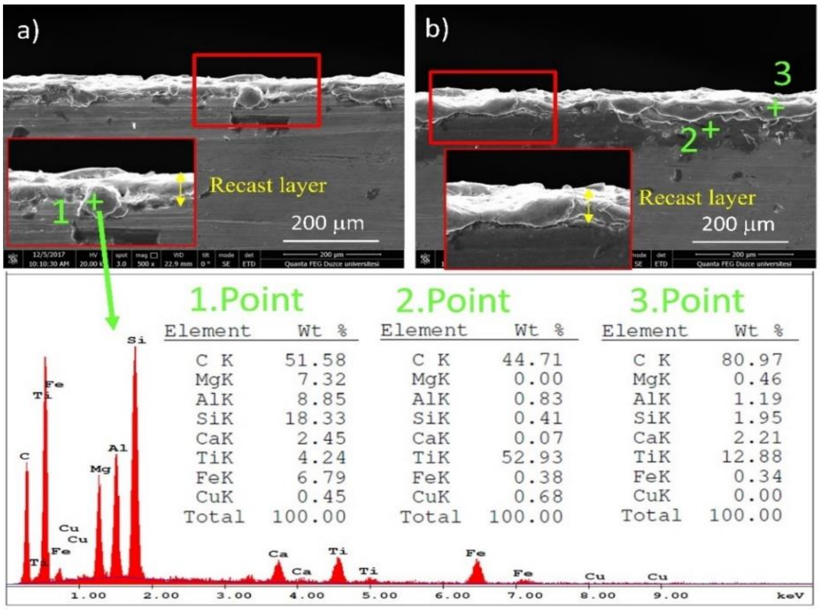

Fig. 4 SEM view of test specimen cross-sections and EDAX analysis: a) 1.Exp., b) 3. Exp.

3.4 Analysis of signal/noise ratio

The Taguchi DOE was used to carry out the EDM tests and S/N ratios were applied to optimize the control factors [35]. Table 7 shows the S/N ratios of the resulting data.

Table 7 Input and output parameters of titanium alloy according to L_9 orthogonal array

	Input Parameters			Output Parameters							
Exp. No	Time-on (µs)	Time-off (µs)	Amperage (A)	MRR (g/min)	S/N For MRR	TWR (g/min)	S/N For TWR	Depth (mm/min)	S/N For Depth	Surface Roughness Ra (µs)	S/N For Ra
1	120	40	8	0.00086	61.2808	0.00007044	83.0435	0.00097835	60.1902	3.29	-10.3380
2	120	44	12	0.00177	55.0318	0.00021666	73.2845	0.00197400	54.0931	4.38	-12.8207
3	120	48	16	0.00377	48.4690	0.00047544	66.4582	0.00348653	49.1521	5.40	-14.6416
4	122	40	12	0.00174	55.2134	0.00024428	72.2422	0.00172434	55.2675	4.12	-12.2956
5	122	44	16	0.00374	48.5512	0.00047231	66.5155	0.00253022	51.9368	5.14	-14.2183
6	122	48	8	0.00073	62.7001	0.00006662	83.5280	0.00070872	62.9905	4.06	-12.1788
7	124	40	16	0.00379	48.4343	0.00050604	65.9162	0.00337363	49.4381	5.17	-14.2647
8	124	44	8	0.00082	61.7115	0.00007206	82.8464	0.00075060	62.4918	4.24	-12.5371
9	124	48	12	0.00152	56.3655	0.00021982	73.1588	0.00095572	60.3934	4.61	-13.2813

The S/N ratios and main effect plots for MRR, TWR, depth, and surface roughness are shown in Fig. 5. The lowest value for MRR (16 A, 124 µs time-on, and 40 µs time-off) was determined to be 0.00377 g/min. The lowest wear loss for TWR (8 A, 120 µs time-on, and 40 µs time-off) was found to be 0.00007044 g/min. The best depth measurement (16 A, 124 µs time-on, and 40 µs time-off) was 0.00337363 mm/min. The best value for the average surface roughness was 3.29 µm (8 A, 120 µs time-on, and 40 µs time-off). According to the S/N ratios, the most suitable parameter values for MRR were $\mathbf{A_3B_3C_1}$, for TWR $\mathbf{A_1B_3C_1}$, for depth $\mathbf{A_3B_3C_1}$, and for surface roughness $\mathbf{A_1B_1C_1}$.

The effective control factors on the MRR, TWR, depth, and surface roughness values found according to the Taguchi Method are shown in the graphs in Fig. 5, and verify the experimental study results. The most effective parameters on the main effect graphs are indicated by the values nearest to the vertical. The most effective parameter for MRR, TWR, depth, and surface roughness was determined to be amperage. The increase in amperage density leads to more energetic impulses resulting in higher material removal [36]. In the plasma channel, the accelerated ions collide with the workpiece surface. The material is removed from the workpiece due to the kinetic energy of electrons and ions. As the amperage increases, the speeds of the electrons and ions increase, causing their kinetic energy to increase. In other words, as the voltage increases, the kinetic energy increases the MRR [24, 37].

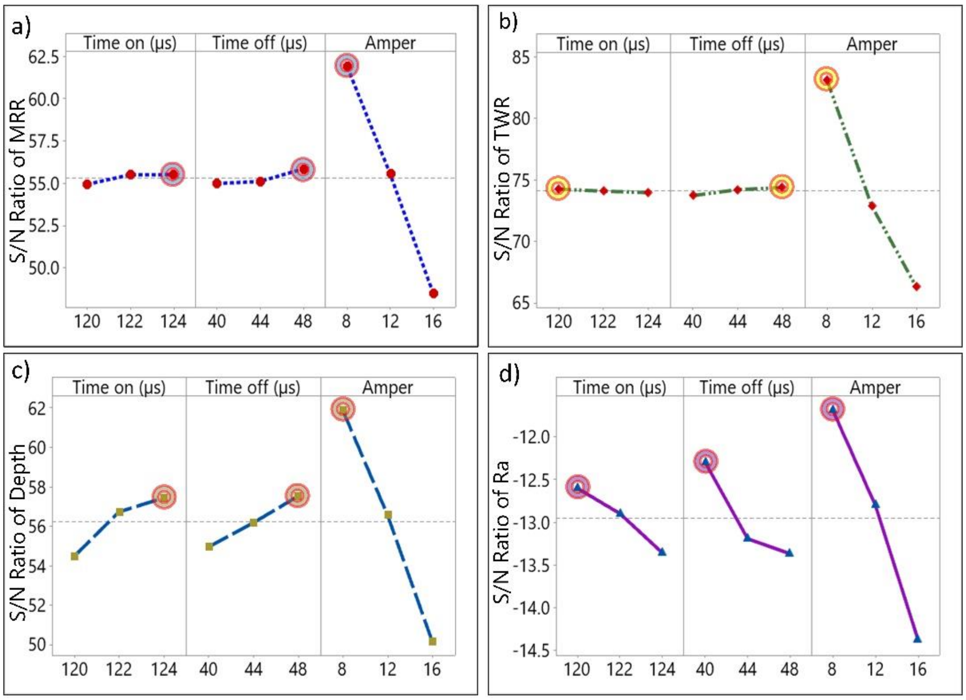

Fig. 5 Main effect plot for S/N ratio for a) MRR, b) TWR, c) Depth and d) Ra

3.5 Anova

Analysis of variance (ANOVA) is used to calculate the significance of the difference between three and more independent means in a normally distributed series. The ANOVA compares cumulative arithmetic means of three or more groups alone. The ANOVA result is also significant when at least one of these comparisons is significant. The effects of time-on, time-off, and amperage on MRR, TWR, depth, and surface roughness were analyzed using ANOVA, carried out at a 95% confidence level and a 5% significance level [38]. The ANOVA results for the MRR, TWR, depth, and surface roughness are shown in Table 8 as **99.66%**, **99.56%**, **87.95%** and **81.12%**, respectively. Therefore, amperage was found to be the most effective factor, according to the contribution percent rates. The wear loss was positively affected by the increase in amperage, while the surface roughness value was negatively affected. The increase in amperage causes the work surface temperature to reach the melting point of the material faster. Thus, more material is removed from the sample surface in constant impact time. As the Time on increases, the average thickness of the white layer increases. The increase in time on causes more thermal energy to be transferred to the surface of the sample during electrical discharge in a single pulse. On the other hand, as the Time on increases, the melted isothermal regions penetrate deeper into the bulk material and the volume of the molten material increases. Thus, the average thickness of the white layer increases and adversely affects the surface roughness [24].

Table 8 The results obtained from ANOVA for MMR, TWR, depth and surface roughness

Material Removal Rate							
Source	DF	Seq SS	Contribution	Adj SS	Adj MS	F-Value	P-Value
Time-on (µs)	2	0.0000000138	0.10%	0.0000000138	0.0000000069	1.66	0.376
Time-off (µs)	2	0.0000000251	0.18%	0.0000000251	0.0000000126	3.02	0.249
Amperage (A)	2	0.0000138805	99.66%	0.0000138805	0.0000069403	1666.44	0.001
Error	2	0.0000000083	0.06%	0.0000000083	0.0000000042		
Total	8	0.0000139279	100.00%				
R-sq: 99.94%			R-sq(adj): 99.76%			R-sq(pred): 98.79%	
Tool Wear Rate							
Time-on (µs)	2	0.0000000002	0.08%	0.0000000002	0.0000000001	1.20	0.454
Time-off (µs)	2	0.0 000000008	0.30%	0.0000000008	0.0000000004	4.47	0.183
Amperage (A)	2	0.0000002632	99.56%	0.0000002632	0.0000001316	1503.96	0.001
Error	2	0.0000000002	0.07%	0.0000000002	0.0000000001		
Total	8	0.0000002644	100.00%				
R-sq : 99.93%			R-sq(adj) : 99.74%			R-sq(pred): 98.66%	
Depth							
Time-on (µs)	2	0.0000004486	4.69%	0.0000004486	0.0000002243	0.84	0.542
Time-off (µs)	2	0.0000001713	1.79%	0.0000001713	0.0000000857	0.32	0.756
Amperage (A)	2	0.0000084095	87.95%	0.0000084095	0.0000042047	15.82	0.059
Error	2	0.0000005317	5.56%	0.0000005317	0.0000002658		
Total	8	0.0000095611	100.00%				
R-sq : 94.44%			R-sq(adj) : 77.76%			R-sq(pred): 0.00%	
Surface Roughness							
Time-on (µs)	2	0.16276	4.57%	0.16276	0.08138	1.74	0.365
Time-off (µs)	2	0.41551	11.67%	0.41551	0.20776	4.44	0.184
Amperage (A)	2	2.88725	81.12%	2.88725	1.44363	30.84	0.031
Error	2	0.09363	2.63%	0.09363	0.04682		
Total	8	3.55916	100.00%				
R-sq : 97.37%			R-sq(adj) : 89.48%			R-sq(pred): 46.73%	

Seq. SS- Sequential sum of squares; Adj. SS- adjusted sum of squares; Adj. MS - adjusted mean squares; F- statistical test; P- statistical val.

3.6 Regression analysis of factors

The extent of the relationship among the variables was measured by regression analysis [39], which was used to calculate the formulae for MRR, TWR, depth, and Ra estimation. The linear models of surface roughness (Ra) estimates are given as (Eqs. 6), (Eq. 7), (Eq. 8), and (Eq. 9), respectively.

$$\mathrm{MRR\ (g/min)} = 0.00114 - [0.000023\mathrm{Ton}] - [0.000015\mathrm{Toff}] + [0.000370\mathrm{A}] \qquad (6)$$

$$\text{TWR (g/min)} = -0.000614 + [0.000003\text{Ton}] - [0.000002\text{Toff}] + [0.000052\text{A}] \quad (7)$$

$$\text{Depth (g/min)} = 0.0139 - [0.000113\text{Ton}] - [0.000039\text{Toff}] + [0.000290\text{A}] \quad (8)$$

$$\text{Ra } (\mu\text{m}) = [-10.04 + 0.0797\text{Ton}] + [0.0625\ \text{Toff}] + [0.1715\text{A}] \quad (9)$$

The regression analysis calculated the VIF (variance inflation factor) = 1. This result showed that the regression model was valid.

3.7 Estimation of optimum parameters

An evaluation was necessary to determine whether the system optimization was sufficiently accurate. The Taguchi approach provided the optimum results. The estimated optimum values for MRR, TWR, depth, and Ra were found *via* (Eq. 10), (Eq. 11), (Eq. 12), and (Eq. 13), respectively.

$$\text{MRR}_\text{P} = \text{T}_\text{MRR} + (\text{A}_3 - \text{T}_\text{MRR}) + (\text{B}_3 - \text{T}_\text{MRR}) + (\text{C}_1 - \text{T}_\text{MRR}) \quad (10)$$

$$\text{TWR}_\text{P} = \text{T}_\text{TWR} + (\text{A}_1 - \text{T}_\text{TWR}) + (\text{B}_3 - \text{T}_\text{TWR}) + (\text{C}_1 - \text{T}_\text{TWR}) \quad (11)$$

$$\text{Depth}_\text{P} = \text{T}_\text{Depth} + (\text{A}_3 - \text{T}_\text{Depth}) + (\text{B}_3 - \text{T}_\text{Depth}) + (\text{C}_1 - \text{T}_\text{Depth}) \quad (12)$$

$$\text{Ra}_\text{P} = \text{T}_\text{Ra} + (\text{A}_1 - \text{T}_\text{Ra}) + (\text{B}_1 - \text{T}_\text{Ra}) + (\text{C}_1 - \text{T}_\text{Ra}) \quad (13)$$

Here, T_{MRR}, T_{TWR}, T_{Depth}, and T_{Ra} indicate the average of MRR, TWR, depth, and Ra values of the experiments. A comparison was made of the estimated values with the verification experiment values for determination of the confidence interval (CI). Equations (Eq. 14) and (Eq. 15) were used to calculate the CI for MRR, TWR, depth, and Ra. The estimated values should be within the 95% CI limit [31]. The symbols used in the CI equations are given in Table 9.

$$\text{CI} = \sqrt{F_{\alpha;1;f_e} x V_e x \left(\frac{1}{n_{eff}} + \frac{1}{r}\right)} \quad (14)$$

n_{eff} formula:

$$n_{eff} = \frac{N}{1+[T_{dof}]} \quad (15)$$

Table 9 Confidence interval (CI) formulae symbols [20]

No.	Symbol	Description
1	$F_{\alpha;1;fe}$	F ratio at a 95% (at F table)
2	α	Significance level
3	f_e	Degrees of freedom of error
4	V_e	Error variance
5	r	Number of replications for confirmation experiment
6	n_{eff}	Effective number of replications
7	N	Total number of experiments
8	T_{dof}	Total main factor degrees of freedom

The average optimal Predict (Pred.) MRR, TWR, depth, and Ra with the CI at 95% was estimated as in (Eq. 16):

$$[(T_{MRR}, T_{TWR}, T_{Depth} \text{ or } T_{Ra})] - [CI] < Pred. < [(T_{MRR}, T_{TWRT}, Th_{Depth} \text{ or } T_{Ra})] + [CI] \quad (16)$$

In order to determine if the predicted experimental result values fell within the 95% CI, the quadratic regression analysis was performed to reveal the relation between the experimental results and the predicted values of the Taguchi optimization. The results of the regression analysis determined that the estimated values fell within the 95% CI limit (Fig. 6).

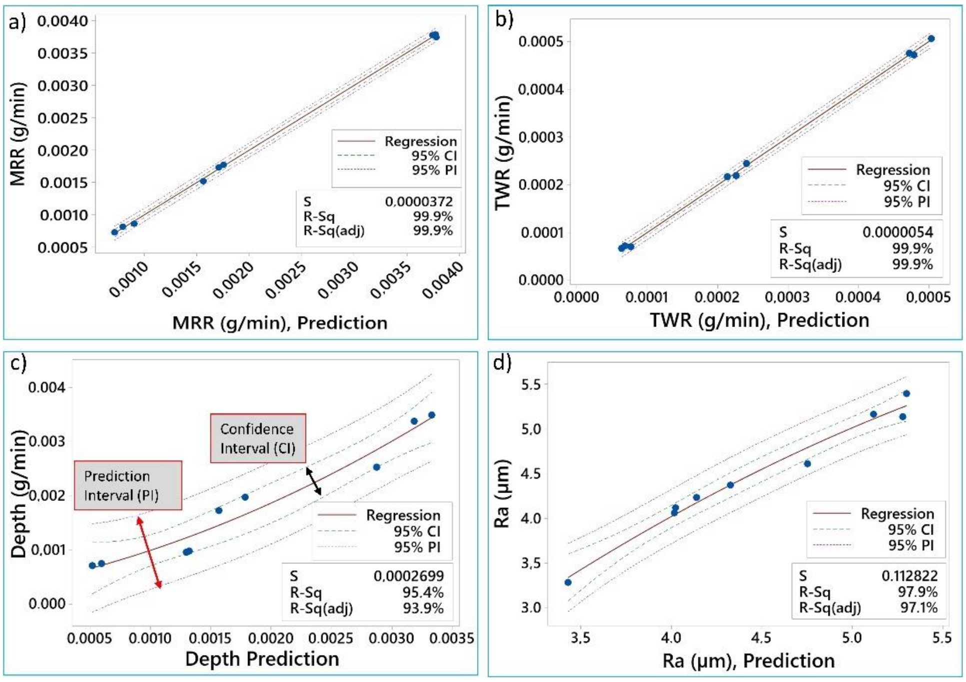

Fig. 6 Comparison of predicted values and experimental results for output parameters, a) MRR, b) TWR, c) depth and d) Ra

4. CONCLUSIONS

This study investigated the parameters (time-on, time-off and A) used in the machining of a titanium alloy on an EDM machine. The results obtained both experimentally and statistically are given as follows:

The best value for MRR was determined to be 0.00377 g/min obtained at 124 µs time-on, 16 A, and 40 µs time-off. The best value for TWR was determined to be 0.0086 g/min obtained at 124 µs time-on, 8 A, and 40 µs time-off. The best value for depth was determined to be 0.00337363 mm/min obtained at 124 µs time-on, 16 A, and 40 µs time-off. The best value for average surface roughness was determined to be 3.29 µm obtained at 120 µs time-on, 8 A, and 40 µs time-off.

- According to the S/N ratios, the most suitable parameter values for MRR were $\mathbf{A_3B_3C_1}$, for TWR $\mathbf{A_1B_3C_1}$, for depth $\mathbf{A_3B_3C_1}$, and for surface roughness $\mathbf{A_1B_1C_1}$.

- According to ANOVA results for MRR, TWR, depth, and surface roughness, the most effective factor was amperage, at 99.66%, 99.56%, 87.95%, and ty81.12%, respectively.
- Increase in the amperage positively affected the wear loss, whereas the surface roughness value was negatively affected.
- The SEM images revealed that the lowest surface roughness value was measured in the first experiment. Increases in amperage values negatively affected the surface roughness and thus, low amperage (8 A) should be chosen for improved surface roughness.

REFERENCES

1. Ghayatadak, M.M., Bhandare, A.S., 2019, *Optimization of electric discharge machining process parameters for H13 steel by using Taguchi method*. In: Sindhwani, K.S.S. (ed.): Advances in Industrial and Production Engineering, Singapore, pp. 525-34. Springer.
2. Yan, B.H., Tsai, H.C., Huang, F.Y., 2005, *The effect in EDM of a dielectric of a urea solution in water on modifying the surface of titanium*, International Journal of Machine Tools and Manufacture, 45, pp. 194-200.
3. Lin, Y.C., Yan, B.H., Chang, Y.S., 2000, *Machining characteristics of titanium alloy (Ti–6Al–4V) using a combination process of EDM with USM*, Journal of Materials Processing Technology, 104, pp. 171-7.
4. Khedkar, N.K., Bongale, A., Kumar, S., Khedkar, V., Kumar, D.V., 2020, *Some investigations on surface quality indicators for OHNS die steel machined with suspended powder EDM process*, International Journal of Machining and Machinability of Materials, 22, pp. 264-80.
5. Ahmadi, M., Karpat, Y., Acar, O., Kalay, Y.E., 2018, *Microstructure effects on process outputs in micro scale milling of heat treated Ti6Al4V titanium alloys*, Journal of Materials Processing Technology, 252, pp. 333-47.
6. Akıncıoğlu, G., Mendi, F., Çiçek, A., Akıncıoğlu, S., 2017, *Taguchi optimization of machining parameters in drilling of AISI D2 steel using cryo-treated carbide drills*, Sādhanā, 42, pp. 213-22.
7. Priyadarshini, M., Pal, K., 2015, *Grey-Taguchi based optimizationof EDM process for titanium alloy*, Materials Today: Proceedings, 2, pp. 2472-81.
8. Verma, V., Sajeevan, R., 2015, *Multi process parameter optimization of Diesinking EDM on Titanium alloy (Ti6Al4V) using Taguchi approach*, Materials Today: Proceedings, 2, pp. 2581-7.
9. Gaikwad, S., Teli, S., Gaikwad, L., 2014, *Optimization of EDM parameters on machining Ti-6Al-4V with a core electrode using grey relational analysis*, International Journal of Research in Aeronautical and Mechanical Engineering, 2, pp. 24-31.
10. Jeavudeen, S., Siddhi Jailani, H., Murugan, M., 2020, *Effect of process parameters in the machining of Titanium alloy and high speed steel in powder mixed electrical discharge machining process*, Materials Today: Proceedings, 27, pp. 615-9.
11. Gaikwad, V.S., Jatti, V.S., Pawar, P.J., Nandurkar, K.N., *Multi-objective optimization of electrical discharge machining process during machining of NiTi alloy using Taguchi and utility concept*. In: Ronge, P.M.P.B.P., Vibhute, R.B.A.S., Apte, S.S. (eds.): Techno-Societal 2018, pp. 479-89. Springer.
12. Nagaraju, N., Surya Prakash, R., Venkata Ajay Kumar, G., Ujwala, N.G., 2020, *Optimization of electrical discharge machining process parameters for 17-7 PH stainless steel by using Taguchi Technique*, Materials Today: Proceedings, 24, pp. 1541-51.
13. Gugulothu, B., Krishna Mohana Rao, G., Hanumantha Rao, D., 2020, *Influence of drinking water and graphite powder concentration on electrical discharge machining of Ti-6Al-4V alloy*, Materials Today: Proceedings, 27, pp. 294-300.
14. Lin, J., Wang, K., Yan, B., Tarng, Y., 2000, *Optimization of the electrical discharge machining process based on the Taguchi method with fuzzy logics*, Journal of Materials Processing Technology, 102, pp. 48-55.
15. Kumar, V., Beri, N., Kumar, A., 2018, *Electric discharge machining of titanium and alloys for biomedical implant applications: a review*, Int JR Anal Rev, 16, pp. 21-32.
16. Nimbalkar, V.S., Shete, M.T., 2017, *Electric discharge machining (EDM) of titanium alloys: a review*, International Journal of Engineering Research & Technology (IJERT), 6, pp. 776-8.

17. Gupta, V., Singh, B., Mishra, R., 2020, *Machining of titanium and titanium alloys by electric discharge machining process: a review*, International Journal of Machining and Machinability of Materials, 22, pp. 99-121.
18. Rengasamy, N., Rajkumar, M., Kumaran, S.S., 2016, *An analysis of mechanical properties and optimization of EDM process parameters of Al 4032 alloy reinforced with Zrb 2 and Tib 2 in-situ composites*, Journal of Alloys and Compounds, 662, pp. 325-38.
19. Kumar, N.M., Kumaran, S.S., Kumaraswamidhas, L., 2015, *An investigation of mechanical properties and material removal rate, tool wear rate in EDM machining process of AL2618 alloy reinforced with Si 3 N 4, AlN and ZrB 2 composites*, Journal of Alloys and Compounds, 650, pp. 318-27.
20. Akıncıoğlu, S., Gökkaya, H., Uygur, İ., 2016, *The effects of cryogenic-treated carbide tools on tool wear and surface roughness of turning of Hastelloy C22 based on Taguchi method*, The International Journal of Advanced Manufacturing Technology, 82, pp. 303-14.
21. Zhang, J.Z., Chen, J.C., Kirby, E.D., 2007, *Surface roughness optimization in an end-milling operation using the Taguchi design method*, Journal of materials processing technology, 184, pp. 233-9.
22. Nalbant, M., Gökkaya, H., Sur, G., 2007, *Application of Taguchi method in the optimization of cutting parameters for surface roughness in turning*, Materials & Design, 28, pp. 1379-85.
23. Masmiati, N., Sarhan, A.A., 2015, *Optimizing cutting parameters in inclined end milling for minimum surface residual stress–Taguchi approach*, Measurement, 60, pp. 267-75.
24. Jabbaripour, B., Sadeghi, M., Faridvand, S., Shabgard, M., 2012, *Investigating the effects of EDM parameters on surface integrity, MRR and TWR in machining of Ti–6Al–4V*, Machining Science and Technology, 16, pp. 419-44.
25. Ekmekci, B., 2007, *Residual stresses and white layer in electric discharge machining (EDM)*, Applied surface science, 253, pp. 9234-40.
26. Lee, H.-T., Hsu, F.-C., Tai, T.-Y., 2004, *Study of surface integrity using the small area EDM process with a copper–tungsten electrode*, Materials Science and Engineering: A, 364, pp. 346-56.
27. Soni, J.S., Chakraverti, G., 1996, *Experimental investigation on migration of material during EDM of die steel (T215 Cr12)*, Journal of Materials Processing Technology, 56, pp. 439-51.
28. Amorim, F., Weingaertner, W., 2004, *Die-sinking electrical discharge machining of a high-strength copper-based alloy for injection molds*, Journal of the Brazilian Society of Mechanical Sciences and Engineering, 26, pp. 137-44.
29. Kumar, A., Kumar, V., Kumar, J., 2013, *Investigation of microstructure and element migration for rough cut surface of pure titanium after WEDM*, International Journal of Microstructure and Materials Properties, 8, pp. 343-56.
30. Puhan, D., Mahapatra, S.S., Sahu, J., Das, L., 2013, *A hybrid approach for multi-response optimization of non-conventional machining on AlSiC p MMC*, Measurement, 46, pp. 3581-92.
31. Sultan, T., Kumar, A., Gupta, R.D., 2014, *Material removal rate, electrode wear rate, and surface roughness evaluation in die sinking EDM with hollow tool through response surface methodology*, International Journal of Manufacturing Engineering, 2014, pp. 2-16.
32. Boujelbene, M., Bayraktar, E., Tebni, W., Salem, S.B., 2009, *Influence of machining parameters on the surface integrity in electrical discharge machining*, Archives of Materials Science and Engineering, 37, pp. 110-6.
33. Hasçalık, A., Çaydaş, U., 2007, *A comparative study of surface integrity of Ti–6Al–4V alloy machined by EDM and AECG*, Journal of Materials Processing Technology, 190, pp. 173-80.
34. Bhaumik, M., Maity, K., 2019, *Effect of electrode materials on different EDM aspects of titanium alloy*, Silicon, 11, pp. 187-96.
35. Kıvak, T., 2014, *Optimization of surface roughness and flank wear using the Taguchi method in milling of Hadfield steel with PVD and CVD coated inserts*, Measurement, 50, pp. 19-28.
36. Torres, A., Puertas, I., Luis, C., 2015, *Modelling of surface finish, electrode wear and material removal rate in electrical discharge machining of hard-to-machine alloys*, Precision Engineering, 40, pp. 33-45.
37. Yoo, B.H., Min, B.-K., 2010, *Analysis of the machining characteristics of EDM as functions of the mobilities of electrons and ions*, International Journal of Precision Engineering and Manufacturing, 11, pp. 629-32.
38. Sudheer, M., Prabhu, R., Raju, K., Bhat, T., 2013, *Modeling and analysis for wear performance in dry sliding of Epoxy/Glass/PTW composites using full factorial techniques*, ISRN Tribology, 2013.
39. Cetin, M.H., Ozcelik, B., Kuram, E., Demirbas, E., 2011, *Evaluation of vegetable based cutting fluids with extreme pressure and cutting parameters in turning of AISI 304L by Taguchi method*, Journal of Cleaner Production, 19, pp. 2049-56.